WAVELET BASED DISCRETIZATION TECHNIQUE FOR ANALYSIS AND DESIGN OF COMPOSITE STRUCTURES

J. Majak[1], J. Kers[2]*, M. Pohlak[1], M.Eerme[1], K.Luiga[1]
[1] Department of Machinery, Tallinn University of Technology, Estonia,
[2] Department of Material Engineering, Tallinn University of Technology, Estonia,
* Corresponding author(jmajak@staff.ttu.ee)

Keywords: *discretization method, Wavelets, decomposition of the solution*

1. Introduction

During last decade, the Haar wavelet theory has been applied to various problems including image compression, signal processing, solution of differential and integral equations etc. Chen and Hsiao [1] derived a Haar operational matrix for the integrals of the Haar function vector, which is a fundamental result for the Haar wavelet analysis of the dynamic systems. In [2] Hsiao introduced a Haar product matrix and a coefficient matrix. In [1-2] the integral method for solution of the differential equations is used. The highest order derivative included in the differential equation is expanded into the Haar series. Latter approach allows to overcome problems with computing derivatives in the points of discontinuities of the Haar function. The higher order operational matrices and the properties of the corresponding integrals of the Haar functions need still examination. An approach suggested by Chen and Hsiao [1] is successfully applied for solving integral and differential equations in several papers [3-6]. Latter approach is assumed also in the current study. Both, weak and strong formulatin based Haa wavelet discretization methods are discussed. The weak formulation based Haar wavelet discretization method has been introduced by authors of the current study in [5]. Three case studies are considered: free transverse vibrations of the orthotropic rectangular plates of variable thickness in one direction, transverse vibrations of Bernoulli-Euler beam, vibration analysis of wint turbine towers. In order to estimate the accuracy of the obtained numerical solution more adequately, the case studies are chosen so that closed form analytical solution exists in special case. The numerical results corresponding to the special case where the thickness of the plate is constant(case study 1) has been validated against closed form analytical results [7]. The numerical results are compared with the results given in [8] (cas study 1). An analysis of the corresponding discrete systems of algebraic equations has been performed.The possibilities to increase an accuracy of the solution are pointed out. The higher order approximation is proposed. Later approximation is based on decomposition of the solution introduced by authors of the current study in [5]. Recently, the Haar wavelet techniques have been treated for the solution of the PDE-s [9-11]. Numerical results are given for a linearly tapered plate.

2. Haar wavelet family

The set of Haar functions is defined as a group of square waves with magnitude ± 1 in some intervals and zero elsewhere

$$h_i(t) = \begin{cases} 1 & for \quad t \in \left[\frac{k}{m}, \frac{k+0.5}{m}\right) \\ -1 & for \quad t \in \left[\frac{k+0.5}{m}, \frac{k+1}{m}\right) \\ 0 & elsewhere \end{cases}, \quad (1)$$

where $m = 2^j$, $j \in \{0,1\ldots,J\}$, $k = 0,1,\ldots,m-1$. The integer J determines the maximal level of resolution and the index i is calculated from the formula $i = m + k + 1$. The Haar functions are orthogonal to each other and form a good transform basis

$$\int_0^1 h_i(t)h_l(t)dt = \begin{cases} 2^{-j} & i = l = 2^j + k \\ 0 & i \neq l \end{cases} \quad (2)$$

The Haar matrix is defined through Haar functions as

$$H(t) = [h_1(t) \quad h_2(t) \quad ..... \quad h_m(t)]^T . \tag{3}$$

Any function $y(t)$ that is square integrable and finite in the interval [0,1) can be expanded into Haar wavelets. It follows from (1) that the integration of Haar wavelets results in triangular functions. These functions can be expanded into Haar series as

$$\int_0^t H_N(\tau)d\tau \cong P_N H_N(t). \tag{4}$$

The operational matrix of integration P_N is determined by equalizing the left and right sides of the relation (4) in the collocation points $t_1,...t_N$, where $t_l = (2l-1)/(2N)$, $l = 1,...,N$, $t_C = [t_1,..,t_N]^T$ and

$$Q_N(t) = \int_0^t H_N(\tau)d\tau , \tag{5}$$

where $Q_N(t) = [q_1(t),...,q_N(t)]^T$.

As pointed out above, the higher order operational matrices and the properties of the corresponding integrals of the Haar functions need still examination. Let us denote the first order operational matrix and corresponding (first) integrals of the Haar functions by $P_N^{(1)}$ and $Q_N^{(1)}(t)$, respectively ($P_N^{(1)} = P_N$, $Q_N^{(1)}(t) = Q_N(t)$). The second and higher order integrals of the vector of Haar functions $Q_N^{(i)}(t)$ are defined as

$$Q_N^{(i)}(t) = \int_0^t Q_N^{(i-1)}(\tau)d\tau , \quad i => 2 . \tag{6}$$

The vector functions $Q_N^{(i)}(t)$ can be expanded into Haar series similarly to (5). The higher order operational matrices $P_N^{(i)}$ can be evaluated by discretization of integrals of the Haar functions $Q_N^{(i)}(t)$.

3. Case studies

3.1 Free transverse vibrations of the orthotropic rectangular plates of variable thickness

Classical deformation theory is employed. It is assumed that the principal directions of orthotropy coincide with natural co-ordinate system. The equation of motion governing natural vibration of a thin orthotropic rectangular plate is given by

$$D_x\frac{\partial^4 w}{\partial x^4} + D_y\frac{\partial^4 w}{\partial y^4} + 2T\frac{\partial^4 w}{\partial x^2\partial y^2} + 2\frac{\partial T}{\partial x}\frac{\partial^3 w}{\partial x\partial y^2} + 2\frac{\partial T}{\partial y}\frac{\partial^3 w}{\partial y\partial x^2} + 2\frac{\partial D_x}{\partial x}\frac{\partial^3 w}{\partial x^3} +$$
$$+2\frac{\partial D_y}{\partial y}\frac{\partial^3 w}{\partial y^3} + 2\frac{\partial^2 D_x}{\partial x^2}\frac{\partial^2 w}{\partial x^2} + 2\frac{\partial^2 D_y}{\partial y^2}\frac{\partial^2 w}{\partial y^2} + \frac{\partial^2 D}{\partial y^2}\frac{\partial^2 w}{\partial x^2} + \frac{\partial^2 D}{\partial x^2}\frac{\partial^2 w}{\partial y^2} +$$
$$4\frac{\partial^2 D_{xy}}{\partial x\partial y}\frac{\partial^2 w}{\partial y\partial x} = -\rho\gamma\frac{\partial^2 w}{\partial t^2} - kw, \tag{7}$$

where

$D_x = E_x^*\gamma^3/12$, $D_y = E_y^*\gamma^3/12$, $D_{xy} = G_{xy}\gamma^3/12$,

$D = E^*\gamma^3/12$, $T = D + 2D_{xy}$, $E_x^* = \dfrac{E_x}{1-\nu_x\nu_y}$,

$$E_y^* = \frac{E_y}{1-\nu_x\nu_y}, \; E^* = \nu_y E_x^* = \nu_x E_y^* . \tag{8}$$

In (7)-(8) ν , D and E stand for the Poisson's ratio, flexural rigidity and modulus of elasticity, respectively, with subscript corresponding to co-ordinate axis. $w = w(t,x,y)$ is the transverse deflection, ρ is the mass density, $\gamma = \gamma(x)$ is the variable plate thickness and k is the modulus of a Winkler type foundation. In-plane dimensions of the plate are denoted by a and b .It is assumed that the edges of the plate along $y = 0, y = b$ are simply supported, and the other two edges each ($x = 0, x = a$) have clamped or simply supported boundary conditions. The time-harmonic-dependent solution and the Lévi approach are considered. The transverse deflection w can be assumed as

$$w(t,x,y) = w_n(x)\sin(n\pi y/b)e^{i\omega t} , \tag{9}$$

where n is a positive number, ω is the harmonic frequency and $i=\sqrt{-1}$. The system (7)-(8) can be written in terms of non-dimensional variables as

$$W_n^{IV}+\frac{6\bar{\gamma}^2\bar{\gamma}'}{\bar{\gamma}^3}W_n'''+\left[\frac{3(\bar{\gamma}\bar{\gamma}''+2\bar{\gamma}'^2)}{\bar{\gamma}^2}-2\alpha\lambda^2\right]W_n''-\eta\alpha^2\frac{6\bar{\gamma}^2\bar{\gamma}'}{\bar{\gamma}^3}W_n'+$$

$$+\frac{E_y^*}{E_x^*}\left[\alpha^4-\frac{3(\bar{\gamma}\bar{\gamma}''+2\bar{\gamma}'^2)}{\bar{\gamma}^2}\alpha^2\nu_x-\Omega^2\frac{\gamma_0^2}{\bar{\gamma}^2}+12K/\bar{\gamma}^3\right]W_n=0\ , \tag{10}$$

where prime denotes derivative with respect to τ and

$$\tau=\frac{x}{a},\ W_n=\frac{w_n}{\gamma},\ \bar{\gamma}=\frac{\gamma}{a},\ \lambda=\frac{n\pi a}{b},$$

$$\eta=\frac{E^*+2G_{xy}}{E_x^*},\ K=\frac{ka}{E_y^*},\ \Omega^2=\frac{12\rho a^2\omega^2}{E_y^*\gamma_0^2}. \tag{11}$$

In (10)-(11) γ_0 stands for the thickness of the plate at $\tau=0$.

3.2 Transverse vibrations of Bernoulli-Euler beam

Let us consider a linear elastic beam with cross section area $A(x)$ and length $L=L_2-L_1$. The beam is subjected to transverse load $q(x,t)$ measured in positive z direction, the gravity is neglected. The diffential equation of motion is governed by

$$\frac{\partial^2}{\partial x^2}\left(p(x)\frac{\partial^2 w(x,t)}{\partial x^2}\right)-\rho(x)\frac{\partial^2 w(x,t)}{\partial t^2}-q(x,t)=0, \tag{12}$$

where $p(x)$ and $\rho(x)$ stand for the flexural rigidity of the beam and mass per unit length, respectively. In the case of simply supported beam and static analysis the equilibrium equation and boundary conditions can be rewritten in non-dimensional form as

$$\frac{d^2}{d\tau^2}\left(p(\tau)\frac{d^2W}{d\tau^2}\right)-L^4q(\tau)=0, \tag{13}$$

$$W(0)=0,\ \frac{d^2W}{d\tau^2}(0)=0,\quad W(1)=0,\ \frac{d^2W}{d\tau^2}(1)=0. \tag{14}$$

3.3 Vibration analysis of wind turbine twers

The approximate governing partial diferential equation for the bending displacement W of the wind turbine tower/rotor system can be written in the following non-dimensional form [12]

$$\left(EIW_{xx}\right)_{xx}-\left(F_xW_x\right)-P=0, \tag{15}$$

the non-dimensional equivalent distributed load P is givesn as

$$P=-mW_{tt}-g_zW_t+P_{aero}+F_{CTF}\delta(x-1)+M_{TRB}\eta(x-1). \tag{16}$$

In (16), the concentrated tip force F_{CTF} and moment M_{TRB} are transformed to distributed load by the use of the Dirac Delta δ and unit dublet η functions. The distributed aerodynamic force P_{aero} is defined as

$$P_{aero}=4\rho_{air}V_0^2DC_D(x)^{2\alpha_x}(H_0/D_0)f(t), \tag{17}$$

where $f(t)$ is a time-dependent function accounts for the dynamic and gusty nature of the wind, α_x and C_D are the wind shear exponent and the drag coeficient, respectively, V_0 is the wind speed at hub height H_0. The boundary conditions are considered in the form

a) cantilevered end ($x=0$)
   $W=0,\ W_x=0,$
b) free end ($x=1$)
   $\left(-IW_{xx}\right)_x+\left(F_xW_x\right)+M_rW_{tt}=0,$
   $\left(-IW_{xx}\right)-I_r(W_x)_{tt}=0.$

An analysis of the latter problem show that the case study 3 can be considered as special case of case study 2 (i.e. wind tower is modeled by Bernoulli-Euler beam).

4. Discretization technique

According to [2] instead of solution of the differential equation its higher order derivative is expanded into Haar wavelets. In the case of all case studies considered abobe the rank of the higher order derivative $r = 4$ and the approximation used is

$$\frac{d^4 W_n}{d\tau^4} = a^T H_N . \tag{18}$$

In (18) W_n is an approximation for the transverse deflection, a^T and H_N stand for unknown coefficient vector and Haar matrix, respectively.
The solution (18) can be divided into two parts as

$$W_n = W_n^{local} + W_n^{global} , \tag{19}$$

where W_n^{local} and W_n^{global} stand for local and global components of the solution, respectively

$$W_n^{local} = a^T Q_N^{(4)}, \quad W_n^{global} = c_3 \frac{\tau^3}{6} + c_2 \frac{\tau^2}{2} + c_1 \tau + c_0 . \tag{20}$$

The wavelet expansion can be interpreted as element-wise approximation over entire integration domain. The discrete system of algebraic equations for each case study considered can be obtained by inserting the approximation of the transverse deflection in differential equation of motion. Herein the resulting equatins are omitted for consiseness sake. In the case of nonlinear discrete system the following solution procedure can be used in order to reduce the computing time:

a) solution for $N = 1$ (single equation),

b) solution for $N = 2$ taking initial values for the coefficient vector as follows

$$a_1 = a_1(N = 1), \quad a_2 = 0, \tag{21}$$

c) the level of the wavelet is increased twice and the solution is performed for $m = 2^k$ taking initial values for the coefficient vector as follows

$$a_1 = a_1(m = 2^{k-1}), \qquad a_{m/2} = a_{m/2}(m = 2^{k-1}),$$
$$a_{m/2+1} = 0, \ldots, a_m = 0 . \tag{22}$$

The initialisation rules for the coefficient vector suggested in latter solution procedure are justified since the coefficient vector a^T has trend to vanish.

In the case of the discretization method proposed, instead of the weight function, its higher order derivative is expanded into Haar wavelets as

$$\frac{d^2 v}{d\tau^2} = b^T H \tag{23}$$

where b^T stands for the vector of unknown coefficients. Integrating (23) one obtains the weight function as

$$v = b^T Q H , \tag{24}$$

Since the weight function is an arbitrary function, the integration constants in (24) are omitted.

5 Numerical results

In order to evaluate the Haar wavelet based solution the obtained numerical results are compared with corresponding exact solutions and with the numerical results given in [8], etc. In the special case, where the thickness of the rectangular plate is constant the closed form analytical solution exists. Let us consider natural vibrations of the rectangular 5-ply maple plywood plate as an example ($E_x = 1.3147 * 10^5 kg/cm^2$, $E_y = 0.4218 * 10^5 kg/cm^2$, $G_{xy} = 0.1118 * 10^5 kg/cm^2$,). The value of the frequency parameter $\Omega = 48.65$ (first mode - fundamental frequency) corresponding to the exact analytical solution has been achieved for a quite law level of the wavelet ($N = 16$). Furthermore, even values of Ω, corresponding to the level of the wavelet $N = 4$ and $N = 8$ are close to the exact solution. The relative error of the frequency parameter Ω is depicted in Figure 1.

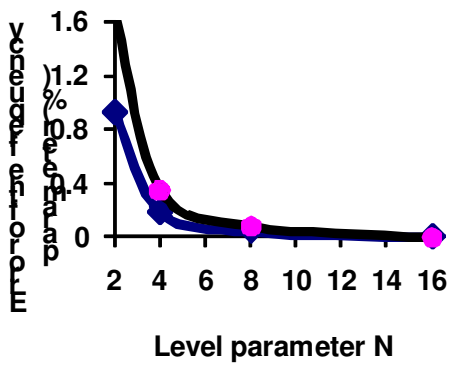

Fig.1. Relative error of the frequency parameter (%). Support regime SSSS.

Upper and lower curves in Fig. 1 correspond to Lal et al. [8] and present solutions, respectively. The relative error of the frequency parameter corresponding to the present solution is smaller, but both errors remain in the same range. Similar behaviour of the relative error can be followed also in the case of boundary conditions where two opposite edges are simply supported and other two clamped.

In Figure 2 the values of the frequency parameter Ω corresponding to the different values of the foundation parameter K are given for orthotropic plate of variable thickness. The nonlinear thickness function is taken equal to $\gamma = \gamma_0(1+\alpha_1\tau+\alpha_2\tau^2)$, where $\alpha_1 = 0.1$ and $\alpha_2 = -0.05$. The foundation parameter K is varied from 0 to 0.02.

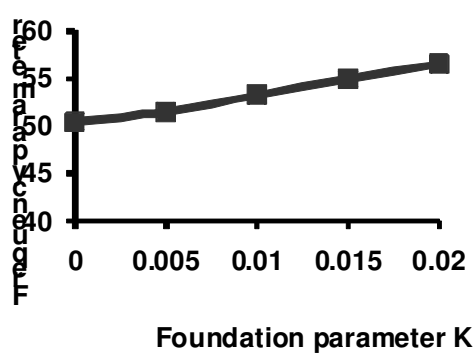

Fig. 2. Frequency parameter for the orthotropic plate of variable thickness (SSSS).

As can be seen from Figure 4 the elastic foundation increases the value of the frequency parameter.

In the case of case study 2 the numerical results obtained using strong and weak formulation based Haar wavelet discretization methods are compared with corresponding results obtained use of FEM and analytical solution. The collocation points are located at the center of the element in the case of Haar wavelet based discretization method (HWDM) and at both ends in the case of used FEM approach. In order to compare FEM and Haar wavelet based discretization methods more adequately, the collocation points of the both methods are included and additional test points (ATP) at distance ¼l and ¾l from end of element (l-element length) are considered as well.The maximum error is estimated as

$$\varepsilon_{\max} = \max_{\tau_i \in X} \left| w(\tau_i) - w^{ex}(\tau_i) \right| , \qquad (25)$$

where X stands for total set of test points. First, the solutions corresponding to strong and weak formulation based Haar wavelet discretization methods coincide in the case of all samples considered. Thus, the numerical results are pointed out for HWDM and FEM (see Table 1).

m	1	2	4	8	16
$\varepsilon_{\max}$ (FEM)	0.00130	0.00012	0.9E-5	0.6E-6	0.5E-7
$\varepsilon_{\max}$ (HWDM)	0.00020	0.6E-5	0.2E-6	0.6E-8	0.2E-9

Table 1. Comparison of maximum errors

As it is seen from Tables 1, the maximal errors corresponding to FEM and HWDM are in the same range. The computations are performed using default accuracy setting in MAPLE 10 (10 digits). The number of elements is varied from 1 to 128, starting from 1 element and by double up elements. A quite small number of elements result in a solution close to the exact one. If the number of elements exceeds

32, the accuracy in range 1E-6 1E-11 is obtained. Evidently, taking use of higher order approximation for the deflection can increase accuracy of the FEM. In current case, the simplest compatible beam element is used. Alternatively, updated discretization scheme can increase accuracy of the Haar wavelet based discretization method.

6. Conclusions

The Haar wavelet based discretization method is adopted for the analysis of the composite structures. The discretization scheme developed has been validated by solving model problems. The obtained results are compared with the results given in [8] (case study 1) and FEM (case study 2). In the special cases, where closed form analytical solution exists, the relative errors of the solution are determined. The complexity analysis of the discrete systems of algebraic equations corresponding to the Haar wavelet based and quintic splines based approaches is performed. The order of the algebraic system is close but lower in the case of the Haar wavelet based approximation. The boundary conditions are satisfied exactly, the solution is approximate in inner points of the integration domain.

Acknowledgement

The support of the Estonian Science Foundation through the grants G8485 is gratefully acknowledged.

References

[1] C.F.Chen, C.H.Hsiao, Haar wavelet method for solving lumped and distributed-parameter systems, in: *IEE Proc. Control Theory Appl*, Vol. 144,pp 87-94, 1997.

[2] C.H.Hsiao, State analysis of the linear time delayed systems via Haar wavelets, *Mathematics and Computers in Simulation*, Vol. 44, 457-470, 1997.

[3] Ü.Lepik, Numerical solution of differential equations using Haar wavelets, *Mathematics and Computers in Simulation*, Vol. 68 (2), pp 127-143, 2005.

[4] Ü.Lepik,: Haar wavelet method for nonlinear integro-differential equations, *Applied Mathematics and Computation*, Vol. 176, pp 324-333, 2006.

[5] J. Majak, M. Pohlak, M. Eerme, T. Lepikult, "Weak formulation based haar wavelet method for solving differential equations". *Applied Mathematics and Computation*, Vol. 211(2), pp 488 – 494, 2009.

[6] J.Majak, M.Pohlak, M.Eerme, Application of the Haar Wavelet based discretization technique to orthotropic plate and shell problems, *Mechanics of Composite Materials*, Vol. 45(6), pp 631 – 642, 2009.

[7] J.N. Reddy, Mechanics of laminated composite plates. Theory and analysis",*CRC Press*, pp 782, 1997.

[8] R.Lal, U.S.Gupta and Reena: Quintic splines in the study of transverse vibrations of non-uniform orthotropic rectangular plates, Journal of Sound and Vibration, Vol. 207(1), pp 1-13, 1997.

[9] LMS.Castro, AJM.Ferreira, S.Bertoluzza, RC.Batra, JN. Reddy, A wavelet collocation method for the static analysis of sandwich plates using a layerwise theory. Composite structures, Vol. 92, pp 1786-1792, 2010.

[10] AJM.Ferreira, LMS.Castro, S.Bertoluzza, A high order collocation method for the static and vibration analysis of composite plates using first order theory, Composite structures, Vol. 89, pp 424-432, 2009.

[11] Ü.Lepik, Solving PDEs with the aid of two-dimensional Haar wavelets, *Computers and Mathematics with Applications* (accepted manuscript).

[12] HM. Negma, KY. Maalawi, Structural design optimization of wind turbine towers, *Computers and Structures*, Vol. 74, pp 649-666, 1999.